

Detection of Fatigue Crack Formation in Glass Fiber Reinforced Thermoplastic Composite with Deep Learning

Fatigue failure and maintenance to prevent its damage causes waste of significant amount of energy, money and workforce especially in areas where mechanical loads occur in high cycles like aviation and automotive industry. Expensive parts are discarded during maintenance to prevent fatigue damage. In particular, discarding high-cost materials like composites results in enormous carbon production and energy waste which are undesirable outcomes in terms of environmental sensitivity. Elium thermoplastic composite is an eco-friendly and recyclable material, low-cost and high strength. Also, its production process decreases the carbon footprint compared to traditional epoxy-based composites. The aim of this project is to determine the region and time of fatigue failure before the damage. For this purpose, three different orientations of Elium thermoplastic composite (0/90, 0/90/45, 45/45) were subjected to fatigue tests at three different tensile strength values (45%, 60%, 75%). The dataset is created with the thermal images that obtained from camera. Machine learning algorithms and CNNs (Convolutional Neural Networks) are utilized on this dataset to predict the region and time of possible failure. As a result of the study, prediction of the location and time of fatigue fracture can be done by using the data collected through the experiments and algorithms.

Keywords: *Elium thermoplastic resin, fatigue fracture, machine learning, convolutional neural networks, infrared thermography*

Introduction

Composite materials have been one of the most important structural materials of our age. This material is used in the most critical sectors because it is very strong, light and expensive. Therefore, it is absolutely very important that the mechanical properties of the products produced using composite materials are predetermined and that there is no chance for damage.

However, composites do not have a homogeneous structure like steels. In the manufacture of a composite product, there are many variables such as composite type, resin type, orientation of fibers, resin to fiber ratio of the part, curing temperature. This makes it difficult to calculate the properties of the product in advance.

It is not possible to determine the mechanical properties of a material with such a complex structure in critical sectors such as aviation, only with mathematical calculations. In this regard, some experiments should be done for each variable of the composite. In this article, experiments were made for elium resin and these experiments were applied in the prediction system with algorithm.

Composite products made using thermoset resins have been on the market for many years. Although thermoset resins are very strong, they are harmful to nature and cannot be recycled. This is why thermoplastic resins have been developed for years. Eventually a thermoplastic resin called elium was developed,

The use of composite products worldwide is increasing year by year. It is estimated that in 2028, the value of products manufactured with composites around the world will exceed 144 billion dollars (Statista, 2022). According to the estimations of OECD, while the total material use in the world was 79gt in 2011, it is predicted that it will increase to 167gt in 2060 (OECD,2018). It can be predicted that the use of composites will increase even more than other materials, since composite materials contain newer and higher technology than other materials.

Europe's recycling and carbon emission standards are getting tighter (EC, 2018). The recycling and emission standards that Europe applies for the entire production sector are a mandatory target for manufacturers. Manufacturers who want their products to be sold to Europe must fulfil these obligations. There is currently no recycling application for composites. However, it is inevitable that the recycling obligation applied to materials such as paper or plastic will also be applied to composites in the future. It is becoming increasingly necessary to use organic matrix composite products.

In addition, fuel consumption and carbon emissions are increasing due to the increasing weight of vehicles. Manufacturers find the solution to this problem by turning the parts of the vehicles into composite materials step by step. In this way, although the carbon emission produced due to weight is reduced, if the part is produced with thermosetting resin, this time it is faced with the European recycling regulations. The solution to this is composite parts produced with recyclable thermoplastic resin.

This is a new resin and has many advantages. Some tests need to be done to measure the levels of these advantages. Elixir is a resin with many types besides its advantages. Different types can be preferred according to the area and sector to be used (Arkema). Elixir has 12 types according to the manufacturer Arkema and is suitable for all composite manufacturing methods such as RTM, pultrusion, hand layup.

Literature Review

Mechanical Features of Elixir

Elixir is a thermoplastic composite with many extraordinary features. It has many mechanical advantages compared to traditional carbon/epoxy composites. Tensile tests of material are made in Istanbul Technical University and according to report in 2020 Elixir's UTS varies highly according to its fiber orientation but it can go as high as 610 Mpa. The detailed Tensile test results are given in Table 1 According to study of Bhudolia et al., Elixir 21%

lower loss in structural integrity, Higher strain to failure for carbon/Elum® composite under flexure. 21.7% higher structural damping for carbon/Elum® composite tube.

Table 1. *Condition Table of Orientations*

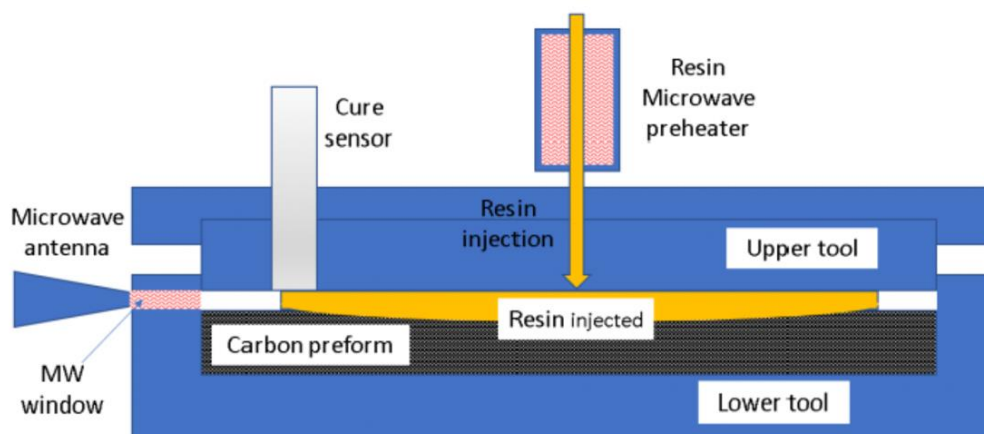
Orientation	UTS (MPa)	Elastic Modulus (GPa)	Elongation at Break (%)	Weathering Test Conditions	
0/90/45	402,8	7,5	5,5	23 °C – 88 h – 50% RH	E1
0/90	616,9	11,3	7,1		
45/45	193,3	2,2	27,7		

And according to different study that made in 2021 also by Bhudolia et al, Carbon/Elum® composite has shown 170% higher absorbed energy and 70% higher major damage energy compared to Carbon/epoxy composite (Bhudolia et al, 2020).

Production of Elum Thermoplastic Composite

Beside mechanical advantages of Elum, one aspect puts forth specifically, unlike other thermoplastic composites due to its very low viscosity Elum can be injected in room temperature easily. Production scheme of Elum can be seen at figure below. Production procedure is relatively simple. First mold is filled with liquid epoxy then the injected epoxy cured and solidified by microwave, molds are mostly steel. Since Elum® resins are available in a range of viscosities between 100 and 500 cps at 25°C (Pantelilis et al, 2019), this process can be taken place in any normal environment. Thermoplastics are highly recyclable and because of Its mechanical features, low energy requirement and high recyclability makes Elum top notch green material that can replace aluminum and many more.

Figure 1. *Production Process*



Fatigue of Composites

Composites are one of the main materials that is used in aviation industry and aviation is a field where high cyclic loads, vibration and fatigue occur. Since that is the situation fatigue of composites is an important subject to study. In his book Kaw stated “Applied stress, laminate stacking sequence, fiber and matrix properties, fiber volume fraction, interfacial bond-ing.” as important factors that effects fatigue of composites (Ziadoon & Chwei, 2016). In Elium the factors are similar. Applied stress and orientation of glass fibers are the most defining parameters to life under cyclic load.

Thermography

Infrared Thermography (IRT), which is also referred to as Thermal Imaging or Simple Thermography in terminology, generates scientific data from dynamic temperature changes in a non-contact way with the help of infrared radiation, which is a type of electromagnetic radiation with long wavelengths that the human eye cannot see. It is a branch of science that is about acquiring information and analyzing, and that can perform non-destructive testing (Usamentiaga et al, 2014).

The main reason why IRT has had a growing interest in the diagnostic and monitoring sector since the beginning of the last century is; commercial infrared or thermal cameras are accelerating in problem solving, sensitivity and speed, and are increasingly being sold at affordable prices. It distinguishes itself from traditional detection methods, both with its measurements and with the fact that it is a method that can be used repeatedly after anomaly detection. In other words, IRT; It is the preferred imaging method for temperature mapping of an object. Biology, construction, aviation, cultural heritage, etc. It is widely used (Czichos, 2013).

Infrared radiation emission is inevitable for all objects above the absolute zero point ($T > 0$ K). Infrared measuring devices can only convert the radiation into an electronic signal, thanks to the propagation of this type of radiation by the objects. These outputs are translated into a detailed infrared image of the instant scene by a series of sensors in the measuring device (Modest, 2013).

The advantages of this science are:

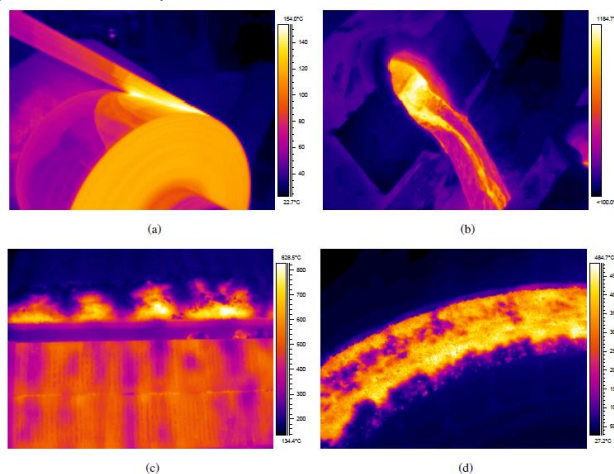
- It is a non-contact observation area; All appliances are located away from the heat source. In this way, even the temperature of dangerous substances containing high heat such as acid can be measured, keeping the user away from danger.
- IRT is not invasive. It does not interact with the target in any way, it does not go over it.
- Having a fast observation rate shortens the waiting times of wasted non-working. In addition to high-speed scanning of stationary objects, it can also acquire data from fast-moving objects and rapidly changing thermal patterns.

- Provides two-dimensional thermal images that enable comparisons between regions of interest.
- As with derivative technologies, it is not exposed to the harmful effects of radiation (see X-ray imaging, etc.).
- It is beneficial that its applications are diverse and abundant.
- Viewing capacities have improved as their output is in visual and video format. The results are more convenient for interpretation than other methods.
- It provides success in examinations that are difficult to perform in other non-destructive examinations, thanks to examination kits specific to some examinations (Gade, Moeslund, 2014).

The disadvantages are:

- The principle of homogeneously addressing common surfaces with a significant amount of energy in a short time.
- Equipment costs are a concern because affordable cameras are not accurate enough. Camera types will be discussed again in the following sections.
- Method out of operation except for “changing thermal properties” in part measurement metrics.
- Ability to probe to a limited thickness below the surface.
- Low emissivity materials can often reflect thermal radiation from the environment. In order to increase material emission, surface paint can be preferred or materials with high emission values should be examined.
- Thermal image degradation due to thermal losses (Meola, 2012).

Figure 2. *Dynamic temperature changes in different utilizations: (a) Temperature measurement in steel strip; (b) Temperature measurement in pig iron; (c) Temperature measurement on sintered material; (d) Temperature measurement from rotatory cooler.*



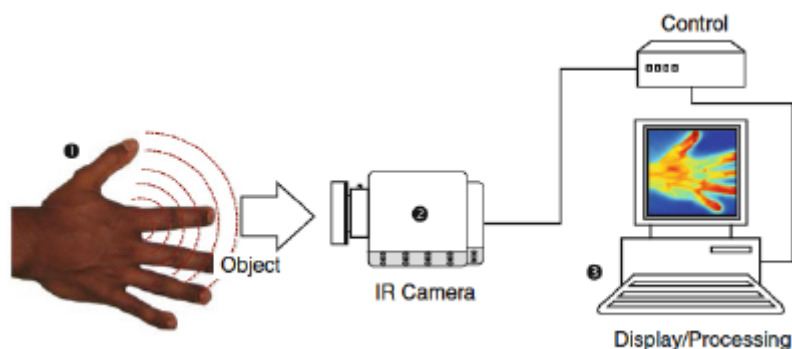
Source: Sensors, 2014.

Approaches in Thermography

Infrared Thermography is studied in two different approaches: passive thermography, where materials and structures are located at different temperatures in the environmental environment, and active thermography, which requires external stimulation for thermal contrast (Maldague, 2001).

In passive thermography, the object or system (1) having a unique thermal contrast with respect to the environment can be viewed using an infrared camera (2). In addition, images can be displayed and processed with the help of a control unit and a computer system (3) when necessary. There is passive thermography setup as follows.

Figure 3. Passive Thermography Configuration



Source: Czichos, 2013.

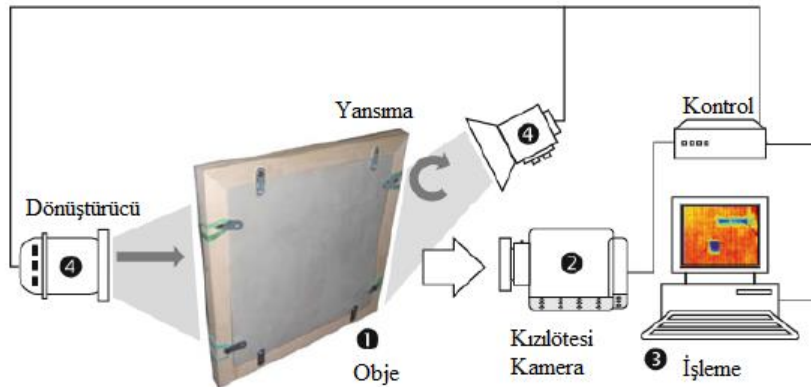
Diagnosis of the abnormality or the presence of the hotspot is one of the aspects that make the passive approach qualitative. Examination of building humidity, insulation problem, monitoring of electrical and electronic accents under control are among the common usage areas. There are also, unlike others, highly innovative potential quantitative passive thermography applications such as the investigation of civil engineering structures using solar loading, water ingress detection on landing aircraft, and automatic human screening on suspicious human behaviour identification.

Active thermography has widespread uses in the field of non-destructive testing, since any form of energy can be used, provided that the thermo-physical properties for imperfect and perfect areas are different enough to produce measurable thermal contrast.

Their experimental configuration is similar to the passive approach. The energy source (4) is required to create thermal contrast in the system (1). The energy source can be placed on the side of the camera (2) (reflection) or opposite the camera (transmission). The control unit is required to synchronize the energy source and the data acquisition part. The computer system (3) undertakes the task of displaying and processing the images. Signal processing in active thermography is essential for quantification and contrast enhancement.

There is an active thermography setup as follows.

1 **Figure 4. Active Thermography Configuration**



2 Source: Czichos, 2013.

3
4
5 Generally, reflection type heating devices are the most suitable method for
6 detecting defects located close to the heated surface. On the other hand,
7 transmission assemblies are more suitable for detecting defects close to the rear
8 surface due to the spreading effect of the thermal surface.

9 In addition, different applications are also available. For example; If the part
10 is hollow, it may be preferable to stimulate it from the inside with a flow of liquid
11 or gas. In this setup, variation in yield temperature can cause abnormal variations
12 in wall thickness or blocked passages due to delayed thermal degradation.

13 Data Processing in Infrared Thermograph

14 Artificial Neural Networks

15
16 The main purpose of this topic is the processing technique that started to be
17 applied in the field of INDT (Infrared Non-destructive Testing) of Thermography,
18 rather than examining neural networks. By targeting defect progression and
19 detection, the main preference is to achieve automatic data interpretation (Almond
20 & Lau, 1994).

21
22 Biologically inspired by the anatomy of the brain and its architecture, this
23 robust and adaptable method emerges from a rather simple idea; A neuron is like a
24 cell with several inputs (x_1, x_2, \dots, x_n) and one scalar output (y). The neuron
25 multiplies the inputs with the weights (w_1, w_2, \dots, w_n), and the product products
26 are linearly combined.

$$27 \quad S = x_1w_1 + x_2w_2 + \dots + x_nw_n \quad (1)$$

28 The output signal y is not significant unless it reaches a certain T threshold, which
29 fires the neuron. The output signal is simply expressed as:

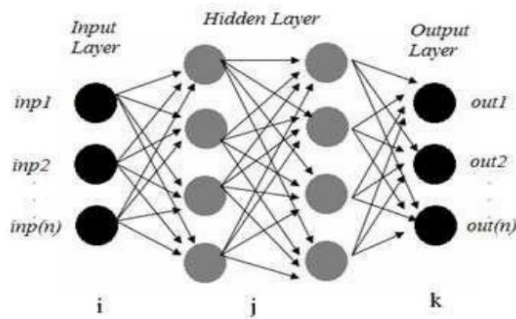
$$30 \quad y = f(S - T) \quad (2)$$

31 From this single building block neuron, various architectures are possible,
32 with many layers of neurons, feed-forward and feedback systems, and supervised
33 or unsupervised learning [Learning: determining values for weights (w_i)] (Benitez
34 et al, 2007). Also, many groups today are now implementing diagnostic tools
35 based on neural networks.

Machine Learning and Algorithm Model

Neural networks, also known as artificial neural networks or simulated neural networks, are a subset of machine learning that provide the foundation of deep learning techniques. Their name and structure are derived from the human brain structure and they resemble the way biological neurons communicate with one another. A node layer contains an input layer, one or more hidden layers, and an output layer in artificial neural networks. Each node, or artificial neuron, is connected to the others and has a weight and threshold linked with it. If a node's output exceeds a certain threshold value, the node is activated, and data is sent to the next tier of the network. Human brain has 10% error rate in general but if neural networks are to be used this error rate would be down near to 5% and that is why artificial neural networks is selected to be consulted.

Figure 5. *Neural network architecture*



Source: Razzak et al 2018.

In order to achieve meaningful conclusions from the data, the application of Deep Learning (Machine Learning sub-branch) is chosen for making anomaly detection. Predictive maintenance is a branch of anomaly detection and is the main goal to proceed in this study. Through predictive maintenance, it is aimed to predict the crack time before the fatigue crack occurs.

Image processing is preferred to utilize in terms of processing and interpreting the data, more than machine learning. Though conventional ML algorithms for image rendering are much more reliable, in this application for image learning, there is a strong requirement of tightly knit pixel-based features to be extracted. Unfortunately, conventional methods become inefficient in this type of study.

Under Deep Learning Methods, due to being the most efficient network to process pixel-based frame data, Convolutional Neural Networks (CNN) is chosen to utilize with visual data for processing the pre-processed mechanically driven active thermographic images.

CNN

There are numerous neural networks according to usage in different situations, one of the widely used neural networks is Convolutional Neural

1 Networks (CNN). Convolutional Neural Networks is preferred for processing data
2 such as visual or audio signal inputs, as it is known for its superiority. The most
3 important 3 layers of CNN's are:

- 4
- 5 • Convolutional layer
- 6 • Pooling layer
- 7 • Fully-connected (FC) layer
- 8

9 Convolutional Layer

10 The convolutional layer is the most important component of a CNN since it is
11 where the majority of the processing takes place. It requires input data, a filter, and
12 a feature map, among other things. Let's pretend the input is a color picture, which
13 is made up of a 3D matrix of pixels. This implies the input will have three
14 dimensions: height, width, and depth, which match the RGB color space of a
15 picture. A feature detector, also known as a kernel or a filter, will traverse over the
16 image's receptive fields, checking for the presence of the feature. Convolution is
17 the term for this procedure.

18

19 Pooling Layer

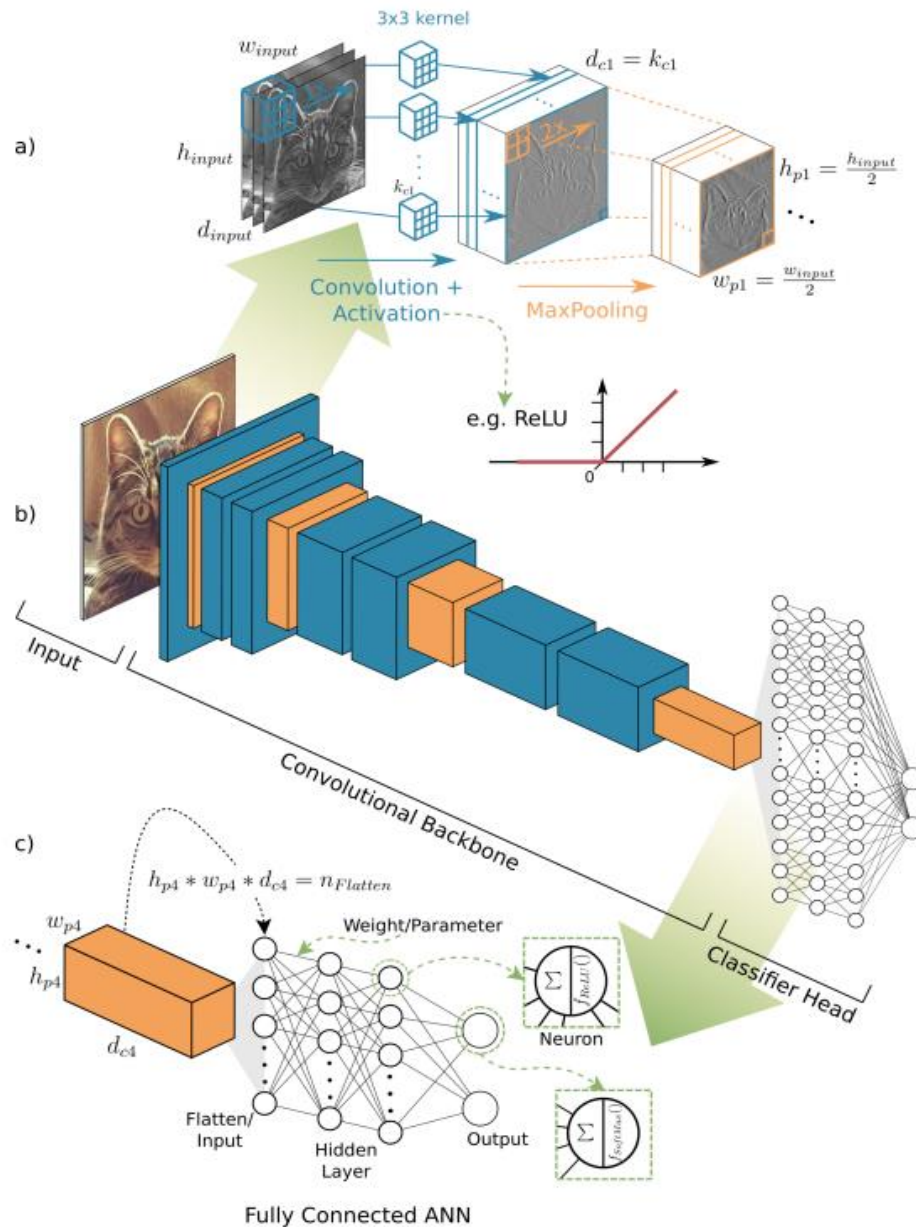
20 Pooling layers, also known as down sampling, reduces the number of
21 parameters in the input by performing dimensionality reduction. The pooling
22 process, like the convolutional layer, sweeps a filter across the whole input. While
23 the pooling layer loses a lot of information, it does provide a few advantages for
24 the CNN. They assist in reducing complexity, increasing efficiency, and reducing
25 the danger of overfitting.

26

27 Fully-Connected Layer

28 The layer where pixel values and input images that are not directly connected
29 to each other are connected to the output layer. The task of this layer is to extract
30 features from previous layers and different filters and features used in those layers
31 (Moreno, 2019).
32

1 **Figure 6. Conventional Convolutional Neural Network Architecture**

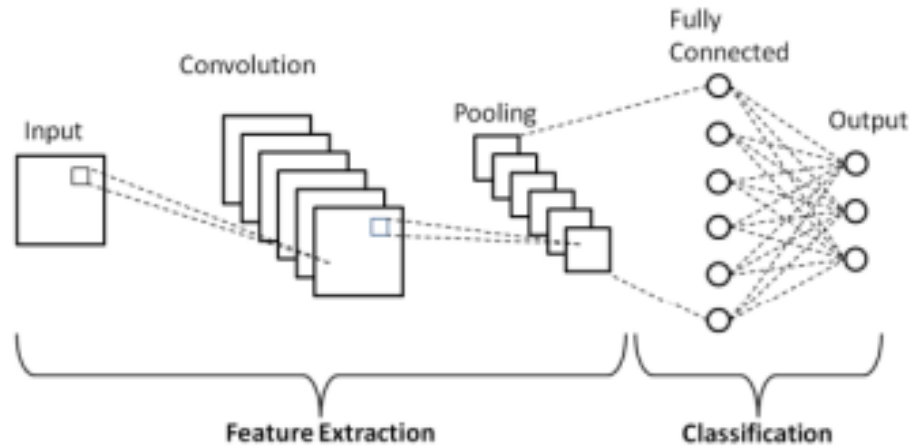


Source: Hoeser & Kuenzer, 2020.

A convolutional neural network (CNN) architecture for image recognition is described in depth; (a) Zoom in on a three-channel RGB input using convolution + activation, such as Rectified Linear Unit (ReLU) (blue), and neighboring max pooling processes (orange). Those processes are repeated in (b) the convolutional backbone, which is part of the architecture's overall structure. Convolution creates feature maps from an input image, which are then scaled by max pooling operations, resulting in reduced resolution but deeper feature maps until they reach a classifier, the architecture's brain, in this case a fully connected artificial neural network (ANN). (c) Information on the transition from the convolutional backbone to the classifier head, as well as the

1 construction of a multi-layer ANN that performs classification (Benitez et al,
2 2007).

3
4 **Figure 11.** *Basic Convolutional Neural Network Diagram*



5
6 *Source:* Phung, & Rhee, 2019.

7
8 As shown in the figure, CNNs are attachable and customizable models.
9 Either feature extraction or classification part can be changed as much as the
10 specialist developer wants. In this study, the model will be optimized just
11 enough to maximizing the accuracy until the end of healthy accuracy threshold.
12 Otherwise, the model can overfit the data. The last fully optimized model has 5
13 layers of Convolutional and Pooling layers, one layer of Flatten layer and 2
14 layers of Dense layers. The activation layer has been selected as, Rectified
15 Linear Unit Function (ReLU). Due to the classification of this study has two
16 outputs, the output activation layer is selected as the Sigmoid Function.

17 18 19 **Methodology/Materials and Methods**

20 21 *Fatigue Test for Elium*

22
23 In general fatigue tests are runned for determining the fatigue life of
24 materials under certain stress, that stress usually chosen as the percentage of
25 Ultimate Tensile Strength (UTS) of material. But in this study our main
26 purpose is not determining life of specimen, we aim to determine where and
27 when the failure going to occur. In this aim different methods of crack
28 detection have been tried. There are studies that is made on metals to detect
29 internal cracks (Usamentiaga, 2014). In these studies, metal plates are heated in
30 one direction and the ups and downs in heat is considered as cracks, since
31 Elium is an insulating material heating method has not given meaningful
32 results. So different method had to be tried. So new experiment setup has been
33 prepared. First 5x15x200 mm specimens are cut from plates with help of table
34 saw.

1 **Figure 12.** *Preparation of specimen*



2
3
4 Then prepared specimens are carefully mounted in fatigue test machine.
5 Mounting causes most of the problems of procedure since the gripping stress
6 needs to vary according to applied stress and applied stress changes for every
7 orientation because of this most of the 0-90 tests failed at start. As hydraulic
8 press 100 kN Dartec press is used. Whole process is observed with Flir T540
9 Thermal Camera. Whole setup can be seen below. Tests are ran for every
10 orientation (45-45, 0-90, 0-90-45), three times for each orientation. For
11 different tensile strengths of each.

12
13 **Figure 13.** *Experimental Configuration*



14
15
16 The Flir thermographic camera (Flir t540) is selected to save
17 thermographic vision in the tool memory because it is a camera customized for
18 science applications. The camera has 30Hz frequency and has IR resolution of

464 x 348 pixels. Flir t540 as object temperature range between 0° and 650°C degrees.

Due to having extensions of videos as “.csq”, Flir Tools+ program is chosen to cooperate with the camera to inspect thermographic content.

Figure 14. *Flir t40 and its interface*

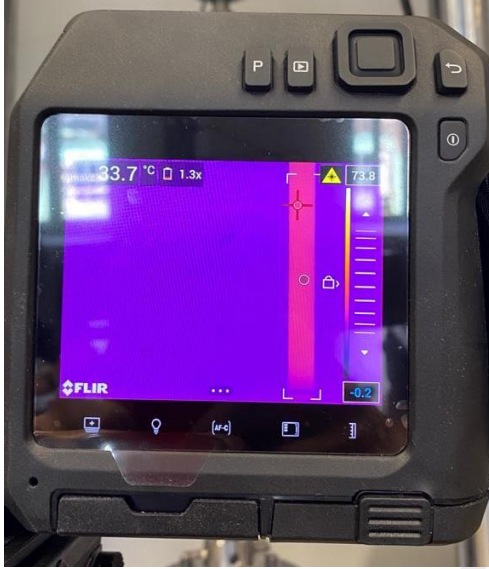
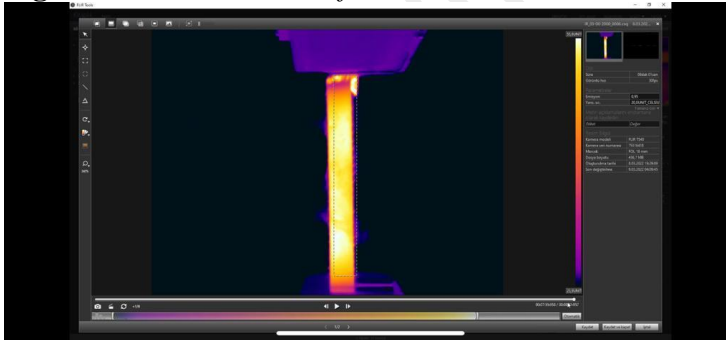


Figure 15. *Flir Tools+ Software*



Data Acquisition

The gathered thermographic data from the camera is stored in its software. The data acquisition system which is chosen to be worked in this study is formed from frames to process in Machine Learning Neural Networks.

Before doing that, the standardization process should be taken into consideration first. There is a critical need for temperature standards due to creating visual thermal distinction in the data. Only by achieving that, image processing will be successful in learning the differences between separate output classes. In order to satisfy this requirement, after information of Ellium heat strength boundaries, a 40°-80°C temperature interval has been selected for

0/90 and 0/90/45 orientations and for 45/45 orientation, due to the strength and yielding processes, 40°- 100°C temperature interval has been selected.

The main aim in this part is dividing gathered thermographic contents which have been held into video format into their own frames. Third party video recording and editing programs have been used to take data from Flir Tools+ and then the conversion has occurred. Only by doing that, will it be possible to talk about the existence of big data in this study.

Figure 16. *The gathered video format content*

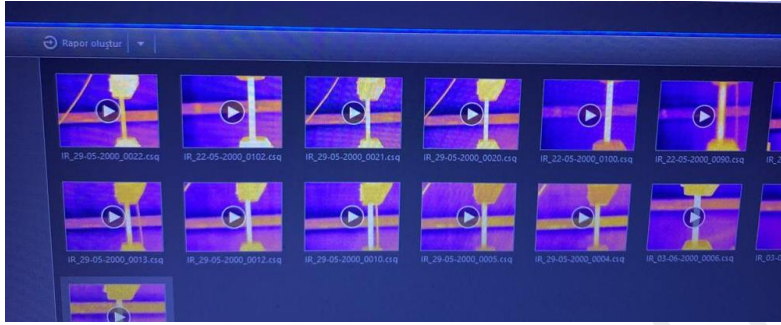
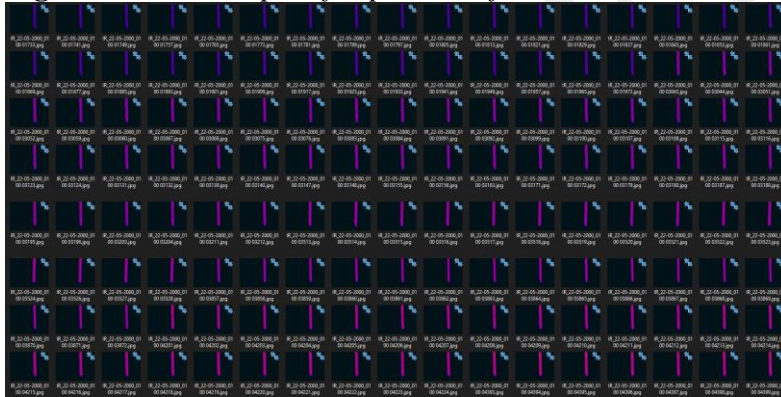


Figure 17. *An example of experiment frames*



After gathering the data together, a meaningful data has to be formed. This phase plays a significant role for efficiency of the algorithm used. After forming a meaningful data from big data, thermal camera data will be ready to cooperate in data processing part.

Model layers are represented below:

1 **Figure 18. Improved Model Summary**

Layer (type)	Output Shape	Param #
conv2d (Conv2D)	(None, 298, 298, 16)	448
max_pooling2d (MaxPooling2D)	(None, 149, 149, 16)	0
conv2d_1 (Conv2D)	(None, 147, 147, 32)	4640
max_pooling2d_1 (MaxPooling2D)	(None, 73, 73, 32)	0
conv2d_2 (Conv2D)	(None, 71, 71, 64)	18496
max_pooling2d_2 (MaxPooling2D)	(None, 35, 35, 64)	0
conv2d_3 (Conv2D)	(None, 33, 33, 64)	36928
max_pooling2d_3 (MaxPooling2D)	(None, 16, 16, 64)	0
conv2d_4 (Conv2D)	(None, 14, 14, 64)	36928
max_pooling2d_4 (MaxPooling2D)	(None, 7, 7, 64)	0
flatten (Flatten)	(None, 3136)	0
dense (Dense)	(None, 512)	1606144
dense_1 (Dense)	(None, 1)	513

2

3

4 **Figure 19. Total Improved Model Parameters**

Total params: 1,704,097
 Trainable params: 1,704,097
 Non-trainable params: 0

5

6

7

8

8 Data Preprocessing

9

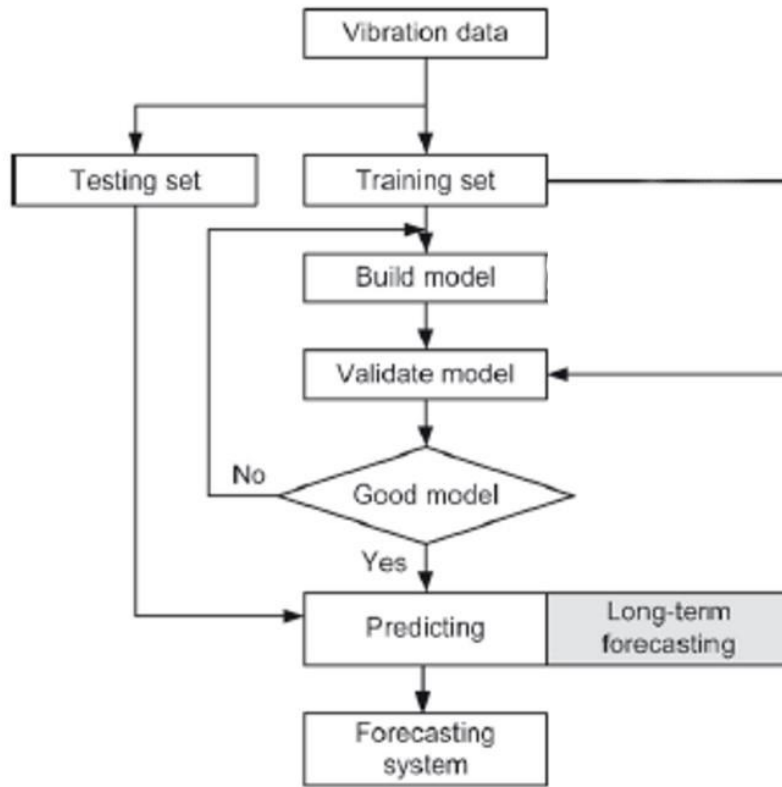
10 Acquired data is split into three forms of dataset; training data, validation
 11 data and test data. This split is required to image processing in the
 12 Convolutional Neural Network. General logic is basically learning an adequate
 13 amount of information and being validated with unknown data to measure total
 14 accuracy. After achieving a high amount of accuracy, the model gets ready for
 15 testing. Test data or test set also has to be different from training data to stay
 16 standardized. General division of data (75% Training set, 20% Validation set,
 17 5% Test set) has been followed (Pham et al, 2010). The current working path of
 18 the project is shown below:

19

20

21

1 **Figure 20.** *Current process path*



2 Source: Pham et al. (2010).
 3
 4

5 **Results**

6 *Fatigue Test Results of Elium*

7
 8 Tests are executed under three different UTS (Ultimate Tensile Strength)
 9 (45%, 60%, 75% UTS) and three different orientation (0/90, 0/90/45 and
 10 45/45). Some of the test results on a small scale are given below.
 11
 12
 13
 14

1 **Table 2. Experiment Result Chart**

Experiment no.	Video name	N	Yönelim	%UTS
402	IR_29_05_2000_0004	11	0/90/45	0.75
403	IR_29_05_2000_0005	58	0/90/45	0.75
404	IR_29_05_2000_0006	411	0/90/45	0.6
405	IR_29_05_2000_0007	FAİL		
406	IR_29_05_2000_0008	FAİL		
407	IR_29_05_2000_0009	FAİL		
408	IR_29_05_2000_0010	797	0/90	0.75
409	IR_29_05_2000_0011	FAİL		
410	IR_29_05_2000_0012	1361	0/90	0.75
411	IR_29_05_2000_0013	413	45/45	0.75
412	IR_29_05_2000_0014	500	45/45	0.75
413	IR_29_05_2000_0015	293	45/45	0.75
414	IR_29_05_2000_0016	465	45/45	0.75
415		FAİL		
416	IR_29_05_2000_0020	1125	45/45	0.60
417	IR_29_05_2000_0021	1058	45/45	0.60
418	IR_29_05_2000_0022	1010	45/45	0.6

As it can be seen in results table there is a strong correlation between orientation and UTS% and N (Cycles till failure). As mentioned above most important results for this test are not revealed by the number of cycles but in thermal camera it was clear to see that failure zone is heated up minutes before failure and failure occurred almost in every time in that zone. Thermal camera images are gathered in camera but it was only observable in Flir tools software so study progressed into importing thermal camera data to software and processing that data with help of thermography.

Models have to be trained, processed and tested separately for each orientation. This is because orientations create different thermal contrasts. Scrambling all the data will dramatically affect the machine's ability to interpret based on orientation. In short, it will confuse the machine.

The data of the 0/90 orientation could not be machined because the infrared thermal data results obtained from the experiments were analyzed and it was unfortunately noticed that the sample in this orientation exhibited a type of thermal response not suitable for visual processing.

Throughout the experiments, 0/90 Elum composite always stays at this (39-42 C) temperature level. The acceleration of the changing thermal contrast is almost zero throughout the experiment. After it reaches 40 C, the external temperature does not increase until the material defect. At the moment of fracture, the inside of the material reaches a temperature of about 65 C, but as it is said, there is no change from the outside, so the subject of visual processing has been interpreted as a distant possibility for this orientation. These constant temperature moments can be explained as stiffness drop.

Accuracy Ratios

Both of the remaining orientations (0/90/45 & 45/45) did not experience the above-mentioned problem, and data with high workability were obtained. Interestingly, training and validation accuracy of over 90% was achieved in both orientations. Ratios are 99% training accuracy and 93% validation

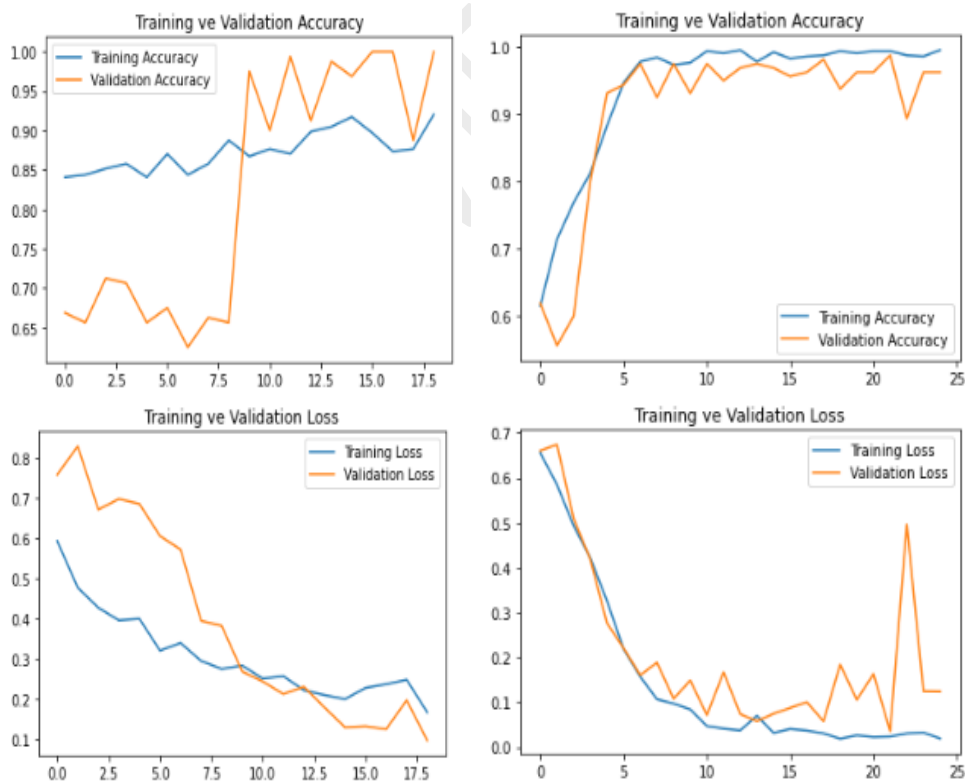
accuracy for 45/45 Elium orientation, and 90% training accuracy and 89% validation accuracy for 0/90/45 Elium orientation.

Figure 21. Model processing iteration results

Orientation	Training	Validation
45/45	loss: 0.0188 - accuracy: 0.9937	val_loss: 0.2483 - val_accuracy: 0.9312
0/90/45	loss: 0.1932 - accuracy: 0.9094	val_loss: 0.1456 - val_accuracy: 0.8938

In order to control the model health, the validation precision was tried not to be too high. Since validation reached “1.00” many times at 0/90/45, the model was stopped before this rate was reached. Below are the graphs of the precision and losses of these models separately, depending on iteration.

Figure 22. Orientation Results (45/45 on the left, 0/90/45 on the right)



Testing the Algorithm

The model may have produced a result that claims to be successful, but if it does not make the right decisions when tried, it will not be successful. For this reason, we tested the machine separately for each orientation, with test data that we reserved before processing.

The main thing that the machine basically learns with convolutions is that it realizes that the material is defective, under 60% to 75% UTS tension, approximately 1-2 minutes before it breaks in the material.

Nearly 100 test data from each orientation are presented to the machine. Although the number of incorrect predictions does not exceed 10, an analog test accuracy of over 90% has been achieved. In addition, it has been determined that some of the wrongly estimated data actually make correct predictions, correct the testers from time to time, and reach a level that can make interpretations with higher precision than the human eye.

Discussion & Conclusion

Elium Fiber Reinforced Plastic (FRP) is extraordinary composite with its mechanical behavior and its eco-friendly features. This study shows that elium thermoplastic composite has a predictable fatigue behavior, especially 0-90-45 and 45-45 fiber orientations. Since its fatigue behavior is predictable, prediction models that is created in this study can be used in industry and practice to prevent damage, loss of energy and even may be human life. Main drawback of this study can be stated as, low samples due to limited time and resources, further studies should be encouraged with larger sample size and more detail.

References

- Statista (2022), Global composites market value 2015-2028
- OECD (2018), Global Material Resources Outlook to 2060.
- EC, 2018, Communication from the Commission to the European Parliament, the Council, the European Economic and Social Committee and the Committee of the Regions — A European strategy for plastics in a circular economy, COM (2018) 28 final.
- Arkema, Liquid thermoplastic resin for tougher composites, www.arkema.com
- Bhudolia, S. K., Gohel, G., Leong, K. F., & Joshi, S. C. (2020). Damping, impact and flexural performance of novel carbon/Elium® thermoplastic tubular composites. *Composites Part B: Engineering*, 203, 108480.
- Pantelidis, N., Bistekos, E., Emmerich, R., Gerard, P., Zoller, A., & Gallardo, R. R. (2019). Compression RTM of reactive thermoplastic composites using microwaves and cure monitoring. *Procedia CIRP*, 85, 249-254.
- Ziadoon, A. H. M. R., & Chwei, Z. (2016). Effect the stacking sequences of composite laminates under low velocity impact on failure modes by using carbon fiber reinforced polymer. *Int. J. Eng. Sci*, 5(2), 53-62.

- 1 Usamentiaga, R., Venegas, P., Guerediaga, J., Vega, L., Molleda, J., & Bulnes, F. (2014).
2 Infrared thermography for temperature measurement and non-destructive testing.
3 *Sensors*, 14(7), 12305–12348. <https://doi.org/10.3390/s140712305>
- 4 Czichos, H. (2013). Infrared Thermography. In *Handbook of Technical Diagnostics*
5 *Fundamentals and application to structures and systems*. essay, Springer Berlin
6 Heidelberg.
- 7 Modest, M. F. (2013). Radiative heat transfer. *Academic Press Inc.*, MA, USA.
- 8 Gade, R., Moeslund, T.B. (2014). Thermal cameras and applications: a survey.
9 *Machine Vision and Applications* 25, 245–262. [https://doi.org/10.1007/s00138-](https://doi.org/10.1007/s00138-013-0570-5)
10 013-0570-5
- 11 Meola, C. (2012). *Infrared Thermography: Recent Advances and Future Trends*;
12 Bentham Science: New York, NY, USA.
- 13 Maldague, X. (2001). In *Theory and practice of Infrared Technology for*
14 *Nondestructive Testing*, Wiley.
- 15 Almond, D. P., & Lau, S. K. (1994). Defect sizing by transient thermography. i. an
16 analytical treatment. *Journal of Physics D: Applied Physics*, 27(5), 1063–1069.
17 <https://doi.org/10.1088/0022-3727/27/5/027>
- 18 Benitez, H. D., Ibarra-Castanedo, C., Bendada, A. H., Maldague, X., Loaiza, H., &
19 Caicedo, E. (2007). Defect quantification with reference-free thermal contrast and
20 artificial neural networks. *SPIE Proceedings*. <https://doi.org/10.1117/12.718272>
- 21 Moreno, R., Gorostegui-Colinas, E., de Uralde, P. L., & Muniategui, A. (2019).
22 Towards automatic crack detection by Deep Learning and active thermography.
23 *Advances in Computational Intelligence*, 151–162. [https://doi.org/10.1007/978-3-](https://doi.org/10.1007/978-3-030-20518-8_13)
24 030-20518-8_13
- 25 Alzubaidi, L., Zhang, J., Humaidi, A. J., Al-Dujaili, A., Duan, Y., Al-Shamma, O.,
26 Santamaría, J., Fadhel, M. A., Al-Amidie, M., & Farhan, L. (2021). Review of
27 deep learning: concepts, CNN architectures, challenges, applications, future
28 directions. *Journal of Big Data*, 8(1). [https://doi.org/10.1186/s40537-021-00444-](https://doi.org/10.1186/s40537-021-00444-8)
29 8
- 30 Razzak, Muhammad Imran, Naz, Saeeda and Zaib, Ahmad 2018, Deep learning for
31 medical image processing: overview, challenges and the future. In Dey,
32 Nilanjan, Ashour, Amira S. and Borra, Surekha (ed), *Classification in*
33 *BioApps: Automation of Decision Making*, Springer, Cham, Switzerland,
34 pp.323-350.